The Effects of Injector Nozzle Geometry and Operating Pressure Conditions on the Transient Fuel Spray Behavior

Ja Ye Koo*
School of Aerospace and Mechanical Engineering, Hankuk Aviation University, Kyunggi-do 412-791, Korea

Effects of injector nozzle geometry and operating pressure conditions such as opening pressure, ambient pressure, and injection pressure on the transient fuel spray behavior have been examined by experiments. In order to clarify the effect of internal flow inside nozzle on the external spray, flow details inside model nozzle and real nozzle were also investigated both experimentally and numerically. For the effect of injection pressures, droplet sizes and velocities were obtained at maximum line pressure of 21 MPa and 105 MPa. Droplet sizes produced from the round inlet nozzle were larger than those from the sharp inlet nozzle and the spray angle of the round inlet nozzle was narrower than that from the sharp inlet nozzle. With the increase of opening pressure, spray tip penetration and spray angle were increased at both lower ambient pressure and higher ambient pressure. The velocity and size profiles maintained similarity despite of the substantial change in injection pressure, however, the increased injection pressure produced a higher percentage of droplet that are likely to breakup.

Key Words : Nozzle Geometry, Operating Pressure, Spray Development, Droplet

1. Introduction

The distribution of fuel in the combustion chamber at the start of combustion is critical to the subsequent combustion. Fuel efficiency and exhaust emissions depend on fuel spray atomization and mixture formation. Better understanding of atomization process and break-up mechanism is necessary to achieve optimum fuel distribution in the combustion chamber for the low pollutant emissions and high engine performance. In the quest for improved emissions, fuel distribution strategies have been changed. Certain techniques have been shown to be effective in reducing certain emissions, for example, high pressure injection in diesel engines is useful for simultaneous reduction of NOx and particulate emissions (Oblander et al, 1989). The break-up of liquid jet is the result of competing unstable hydrodynamic forces acting on the liquid jet as it exits the nozzle (Reitz and Bracco, 1979 ; Shimizu et al., 1990). The behavior of spray, for example, penetration rate, spray angle, and mean drop diameter is governed by the nozzle geometry and up-stream injection conditions as well as relative velocities between liquid and ambient gas, viscous forces, and surface forces (Koo and Martin, 1995 ; Ohrn, 1989). External conditions alone may not be sufficient to explain external spray characteristics. The nozzle geometry and up-stream injection conditions affect the characteristics of flow inside the nozzle, such as turbulence and cavitation bubbles (Ruiz, 1981 ; Wang et al., 1989 ; He and Ruiz, 1995). The cavitation bubbles inside nozzle, which can be produced when the pressure of fuel is lower than the vapor pressure of fuel, is thought to improve atomization efficiency. However, there is lack of knowledge of integrated understanding of internal flow inside nozzle and external spray

* **E-mail** : jykoo@hau.ac.kr
TEL : +82-2-300-0116; **FAX** : +82-2-3158-2191
School of Aerospace and Mechanical Engineering, Hankuk Aviation University, Kyunggi-do 412-791, Korea. (Manuscript **Received** October 16, 2002; **Revised** December 11, 2002)

behavior. In this work an integrated study is carried out, considering of nozzle geometry, internal flow inside nozzle and operating pressure conditions.

2. Experiment Setup and Computer Simulations

Two sets of simplified plain orifices were made for the investigation of the effect of internal flow on external spray. One set is actual scale model of 0.3 mm hole diameter and the other is 100 times scale model of 30.0 mm hole diameter. In the scale model needle was not considered in the orifice, but in the actual nozzle calculation needle was considered. Round and sharp shape of inlet nozzle with various length to diameter (L/d) were tested as shown in Fig. 1. A phase/Doppler Particle analyzer (PDPA) was used in the velocity only mode to measure the fluid velocity at various axial and radial positions inside nozzle. For the external spray, PDPA was also used for the measurement of droplet sizes and velocities. Valid data obtained at each locations were 3000 samples. For the external spay visualization pulsed laser sheet photography system was used as shown in Fig. 2. Computations for the internal flows inside nozzle were carried out for all three geometries- the single-hole diesel injector (L/D=3.3), the simplified single-hole nozzles used in the PDPA and visualization tests, and the corresponding scaled up nozzle. Details for computations are shown in reference (Koo, 1996)

In order to investigate the effect of opening pressure and ambient pressure a single shot injection system was made using solenoid valve as shown in Fig. 3. The opening pressure of dummy injector is 1.1 MPa and the opening pressure of main injector is 20.1 MPa or 40.1 MPa. When the solenoid valve is closed by the solenoid driving pulse fuel is injected through the main injector. The Z-pulse with 5 volts is generated in the rotary encoder that is connected to the shaft of the injection pump every revolution of injection pump. The Z-pulse is the reference pulse in this system. Figure 4 shows Z-pulse signal, external clock, solenoid driving pulse, needle lift and light

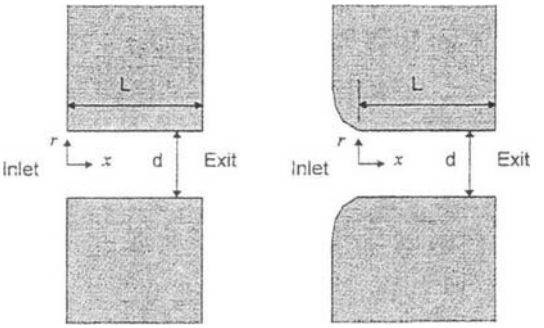

Fig. 1 Sharp and round inlet shapes of the model nozzle

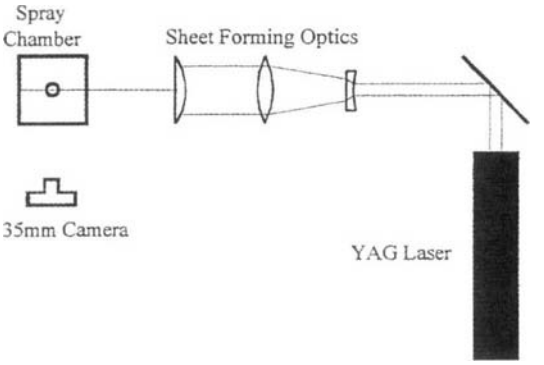

Fig. 2 Schematic of pulsed laser sheet photography system

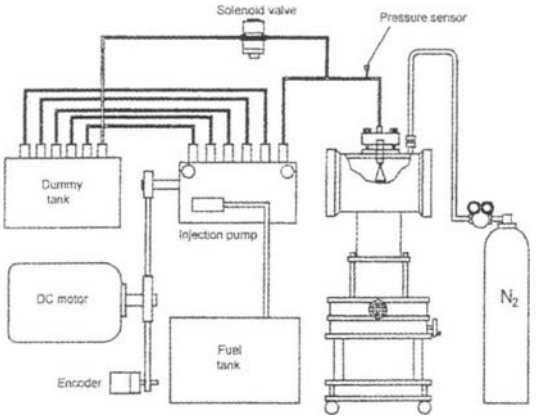

Fig. 3 Schematic of single shot injection system

duration.

In comparing data from two different injection pressures, two different injection systems were used. One is CAV-Lucas injector with a static popping pressure of 15.2 MPa. The nozzle and

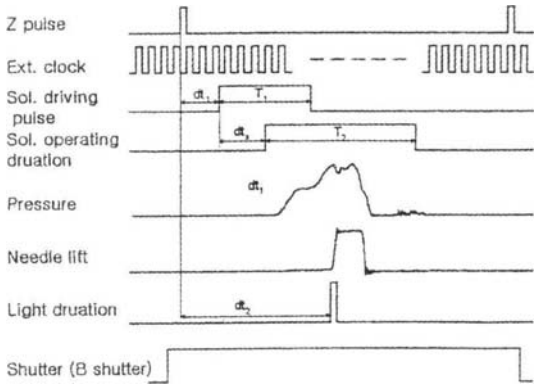

Fig. 4 Control signals for single shot injection system

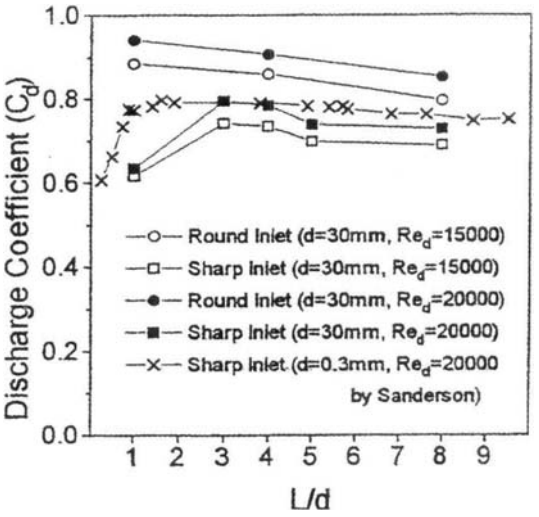

Fig. 5 Variation of discharge coefficient depending on nozzle length to hole diameter

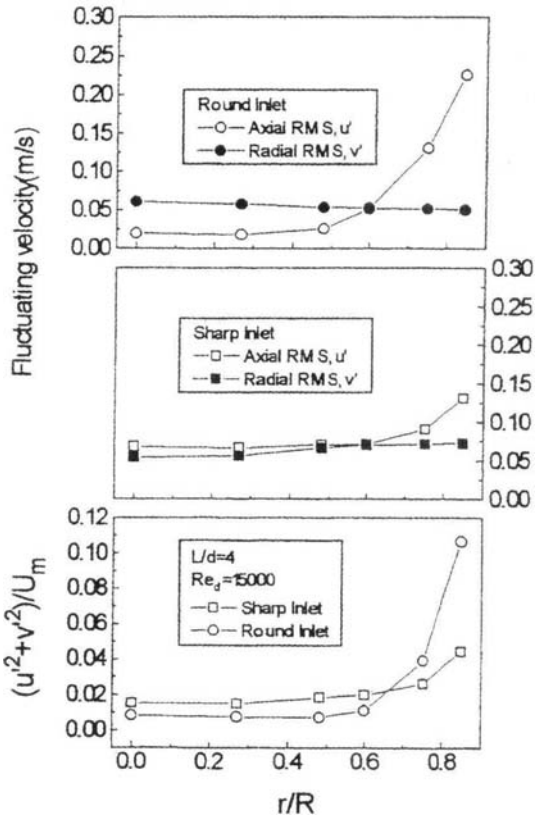

Fig. 6 Variation of turbulent velocities and turbulence intensity at nozzle exit

diameter of the injector were 0.24 mm and 0.8 mm, respectively. This injector was a reference injector used in the calculation of internal flow inside nozzle. The other high pressure injector was Nippondenso EP-9 fuel injection system. The single hole injector was a Nippondenso injector with the same nozzle hole dimensions as in the low pressure injection system. However, the needle opening pressure was 28.6 MPa. The main difference between the two systems is the injection pressure. The high pressure system has a peak injection pressure of 105 MPa while the low injection system has a peak injection pressure of 21 MPa.

3. Results and Discussion

3.1 Effects of nozzle geometry

The discharge coefficients as a function of L/d for a Reynolds numbers of 15,000 and 20,000 for the round and sharp entrance scaled nozzles are shown in Fig. 5. Results of Sanderson for a sharp entrance plain orifice nozzle, as cited by Licharowicz (1965), are included for comparison. As L/d increased for the round inlet nozzle, the discharge coefficient gradually decreased, since the boundary layer remains attached and only grows as the flow develops. The sudden decrease in the discharge coefficient for the L/d=1 sharp inlet nozzle indicate hydraulic flip, because the separated boundary layer reaches the nozzle exit before being able to attach to the wall. The flipped jets emerged from the nozzle as a smooth

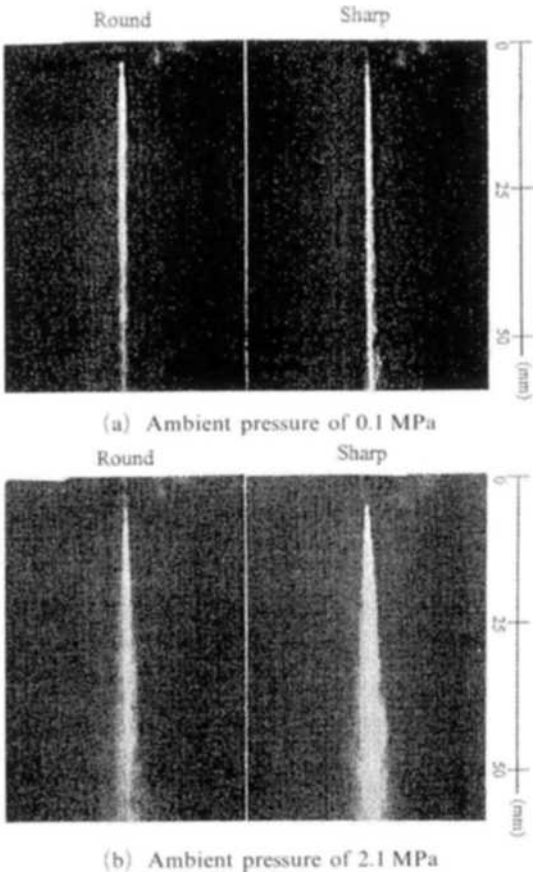

Fig. 7 Spray photographs of round and sharp inlet entrance nozzle

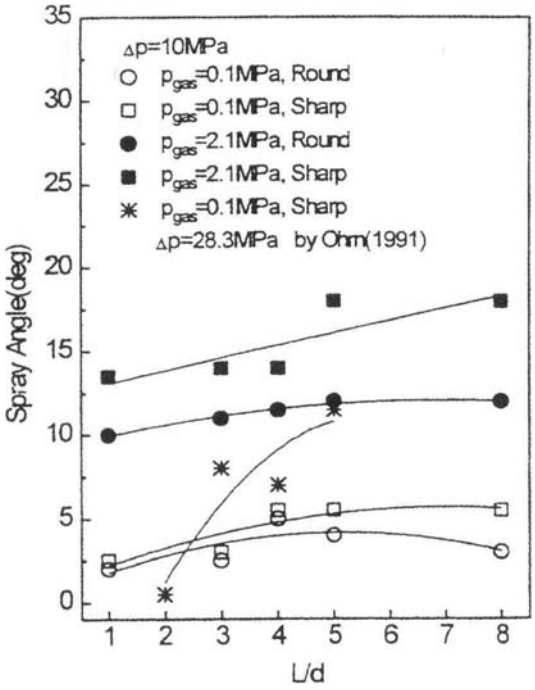

Fig. 8 Effect of nozzle inlet shapes on spray angle at various nozzle length to diameter and ambient pressures

glassy column of fuel which usually slowed and increased in diameter before experiencing a sudden breakup. Figure 6 shows a comparison of measured turbulent velocities and non-dimensional turbulent kinetic energy across the radius of the scaled-up injectors (at the exit) for the L/d=4 nozzles. For the round inlet nozzle, shown in the top plot, the radial fluctuating velocity component at the center is about three times higher than the axial radial fluctuating velocity component, but the axial radial fluctuating velocity component increases from r/R=0.5 out to the wall. For the sharp inlet case the radial component shows the same tendency and value as the round inlet case, but the axial component is significantly higher in the center. As shown in the bottom plot, out to r/R=0.6 (36% of the flow area) the square inlet nozzle flow has about twice the turbulent kinetic energy, compared to the round inlet nozzle. Beyond that point the turbulent kinetic energy of the round inlet nozzle increases very rapidly.

Photographs of the L/d=5 nozzles with round and sharp inlet are shown in Fig. 7 for chamber pressures of 0.1 MPa and 2.1 MPa, in order to see the effect of ambient gas density on external spray characteristics. The injection pressure (Pinj) was 10 MPa. At 0.1 MPa in Fig. 7(a) the sharp inlet and round inlet sprays appear similar because there is little interaction with the ambient gas. At 2.1 MPa in Fig. 7(b) the sharp entrance nozzle results in a wider spray angle, though both are substantially wider than at 0.1 MPa. This shows that the nozzle shape alone does not determine spray shape. Photographs at the same two ambient pressures were taken and the spray angle was measured. Measurements were made from at least five photographs, resulting in a standard error of under +/−2deg, and the average values are shown in Fig. 8. Data of Ohrn (1989) are also

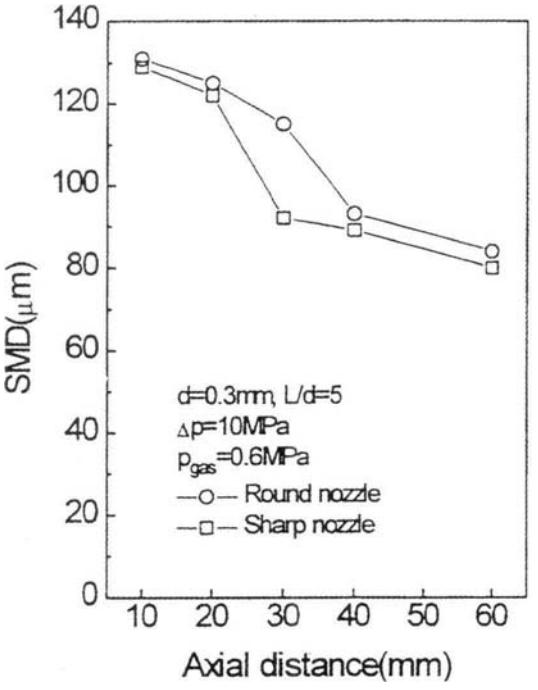

Fig. 9 Effect of nozzle inlet shapes on SMD at various axial distances

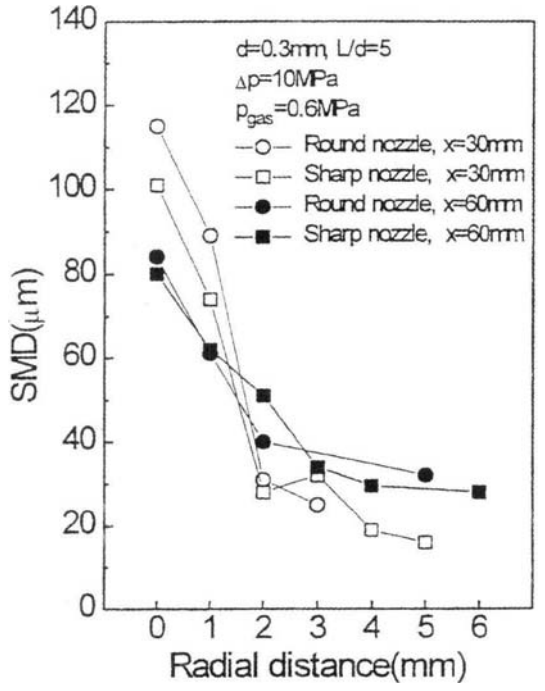

Fig. 10 Effect of nozzle inlet shapes on SMD at various radial distances

included for reference. As a function of nondimensional nozzle length, L/d, the spray angle for sharp entrance nozzle is always wider than the round entrance nozzle, and the gap widens at higher ambient gas pressures.

Figure 9 shows a comparison of Sauter mean diameter(SMD) for L/d=5 round and sharp entrance nozzles at an injection pressure of 10 MPa. The sharp entrance nozzle has a lower SMD at all axial positions. The corresponding radial SMD data for two axial locations (30 mm and 60 mm) are shown in Fig 10. At 30 mm the SMD decrease with radial location except at the 3 mm radial point, which lies outside of the spray. At 60 mm there is no clear difference between the sharp and round inlet nozzles. These two figures show that the sharp entrance nozzle is associated with a smaller SMD, which may be due to higher exit turbulence intensities shown previously for the scaled-up model data and calculation results.

3.2 Effects of opening pressure

Figure 11 (a) shows the photographs at the ambient pressure of 0.1 MPa with opening pressure of 20.1 MPa. A protrusion in front of the spray head can be seen up to the 9 mm development of spray in Fig. 11(a). This protrusion might be injected into the chamber at the opening of the needle from the fuel in the sac volume of the injector. This protrusion is not observed at the high ambient pressure condition as shown in Fig. 11(b). Figure 11(b) shows the photographs

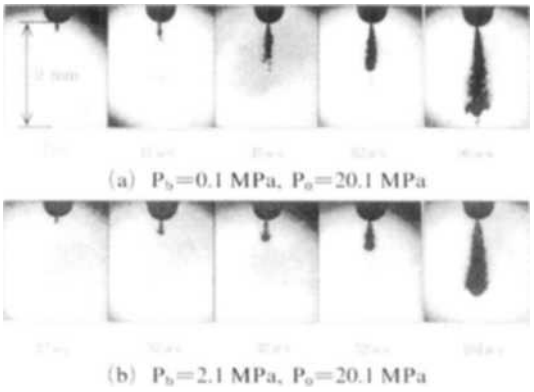

Fig. 11 Early stage of diesel spray at the opening pressure of 20.1 MPa

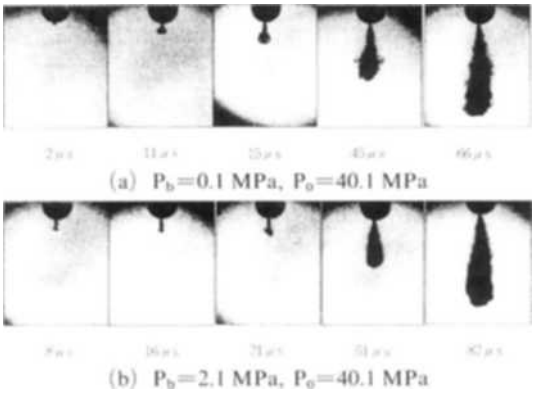

Fig. 12 Early stage of diesel spray at the opening pressure of 40.1 MPa

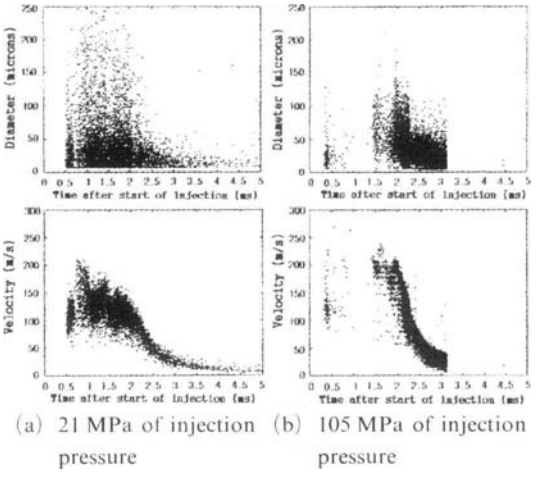

Fig. 13 Transient droplet velocities for the spray axis of 60 mm from the nozzle exit

at the ambient pressure of 0.1 MPa with opening pressure of 20.1 MPa. A mushroom shaped portion can be observed in the spray head at early times at high ambient pressure without protrusion because the fuel in the sac is condensed due to the high ambient pressure and it is injected with the main spray. Figure 12(a) shows the photographs at the ambient pressure of 0.1 MPa with opening pressure of 40.1 MPa. The protrusion is not observed at the high opening pressure condition because the protrusion might be overtaken by high velocity of the main fuel spray. Figure 12(b) shows the photographs at the ambient pressure of 2.1 MPa with opening pressure of 40.1 MPa. A protrusion is not observed in this case. The spray angle seems to be a little narrower than that of 0.1 MPa because the relative pressure difference is reduced.

3.3 Effects of injection pressures

Figure 13(a) and (b) show the velocities on spray axis located 60 mm from the nozzle exit at injection pressure of 21 MPa and 105 MPa, respectively. Data from the low injection spray system for the position of 60 mm from the nozzle exit can be seen in Fig. 13(a). The droplet diameters for the low injection pressure case have large variation ranging from 7.14 μm to 250 μm even though most droplet sizes are less than 75 μm. There are less droplets greater than 75 μm, especially those greater than 200 μm in Fig. 13(a). In viewing the velocity profile, A small gaps of data can be observed in the head of spray due to the high number density of non-sphericity droplet or out of measurable ranges. The wave-like behavior can be seen in Fig. 13(a) with the average velocity in the head of around 140 m/s. In the high injection pressure of 105 MPa, the velocities at the tip of the spray lie chiefly around 125 m/s, lower than the quasi steady portion of the spray behind it, which averages around 190 m/s. In addition, the data gap for the head of the spray has expanded to cover from 0.5 ms after start of injection to 1.5 ms. This data gap expansion to approximately 50% of the head of the spray suggests an increase in droplet number density within the head of the spray. Droplet diameters have redistributed themselves as well. For the most part, drops larger than 125 μm have faded out of existence. This redistribution of large droplets into smaller drops would mean an increase in number density, assuming not many droplets traveled radially outward. The number density increase would explain the data gap. In the tail of the spray, droplets settle into a broad band, ranging from 4.7 to 50 μm. The plots in Fig. 13(b) possess a visible discontinuity within the data. This is a result of the temporal division of the spray into head and tail sections. While somewhat unsightly, this discontinuity does not diminish the validity of the data. It does however present an excellent example of the limited band-

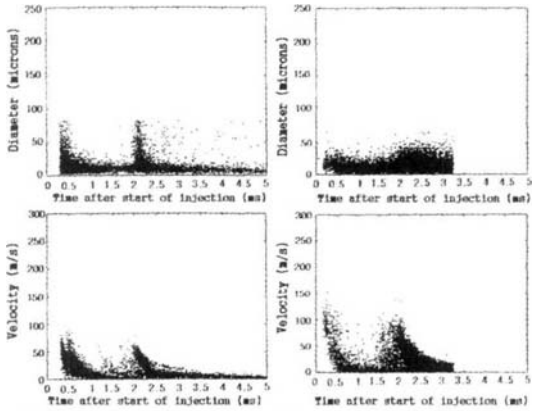

(a) 21 MPa of injection pressure (b) 105 MPa of injection pressure

Fig. 14 Transient droplet velocities for the spray edge of 30 mm from the nozzle exit and 3 mm from the spray axis

width of phase/Doppler instrumentation and how the recorded data is very much a function of the optimization of the instrumentation. Droplet diameters for the high injection pressure have shifted to the lower values less than 100 μm. There are no droplets greater than 150 μm.

At off-axis locations, comparison of droplet diameters proves interesting. Figure 14(a) and (b) show the velocity and diameter profiles for the low injection pressure case and the high injection pressure case, respectively. The plots exhibit double peaks, although the high injection pressure diameter plot's peaks are heavily subdued. The double peaks correspond to the opening and closing of the injector needle. The difference between the two profiles in range of droplet sizes and velocity displayed. As one might expect, the high pressure case exhibits droplets spanning a larger range of velocities than the low pressure case. In the diameter plots, the low pressure case has a greater range for the peaks, but the high pressure maintains a wider range overall.

The droplet data acquired can be compared with droplets breakup criteria to give an indication of the susceptibility of the droplets to aerodynamic breakup processes (Chang and Koo, 1995). The droplet breakup criteria are a function of non-dimensional parameters, specifically the droplet Weber number and the droplet Reynolds number. Following Reitz and Diwakar (1986), the criteria for bag breakup of a droplet is $We_D > 12$. When the criteria $We_D/\sqrt{Re_D} > 0.5$ is met, the breakup process boundary layer stripping (BLS) is assumed to occur. Droplets not meeting these criteria are assumed to be stable. In both the droplet Weber number and droplet Reynolds number calculations, the droplet velocity is the relative velocity with respect to the surrounding gas. Since the velocity of the surrounding gas is an unknown, it is impossible to calculate the true droplet Weber number and Reynolds number. To overcome the lack of knowledge of the true relative velocity of the droplet, two different estimates of relative velocity are made to bound the problem. The first method is to simply use the measured velocity for the relative velocity. This assumes a stagnant gas velocity, making the estimate high in areas where surrounding gas possesses significant velocity from the entrainment process. The second is to assume that the gas velocity is equal to the mean droplet velocity at that point in time and space and take the droplet relative velocity as equal to the absolute value of the droplet velocity minus the average droplet velocity. This method tends to underestimate the relative velocity, but it is more accurate than the first method in areas such as the core of the spray where droplets would have imparted a nonzero velocity to the surrounding gas. The true relative would lie somewhere in between the two estimates.

Figure 15 is a relative velocity-diameter plot of droplet data for the high pressure case at the on-axis location of the 30 mm from the nozzle exit. The plot also includes breakup criteria boundaries for each size class. The bag breakup criterion is represented by solid line, and the boundary layer stripping criterion is indicated by dashed line. The surrounding gas velocity in Fig. 15(a) is assumed to be the average droplet velocity. There are still many droplets larger than 150 μm at this location. The low pressure case does indicate that some droplets would be subject to bag breakup, but there is a few point exceeding the boundary layer stripping criterion. Figure 15 (b) shows several droplets above the bag breakup

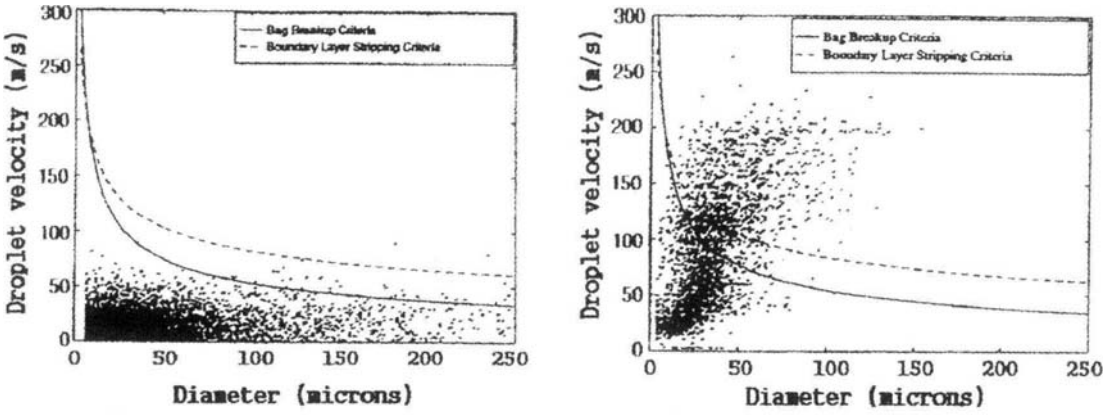

(a) 21 MPa of injection pressure (b) 105 MPa of injection pressure

Fig. 15 Correlation of droplet sizes and velocities for the spray axis of 60 mm from the nozzle exit

and the boundary layer stripping criteria due to the high relative velocity even though the droplet diameter is less than that of lower injection pressure. The droplet relative velocity in this figure is taken as the difference between the droplet velocity and the average droplet velocity for that point in time of the spray. For this location, this method probably gives a better estimate of the true relative velocity. The true relative velocity would likely be somewhat higher, so more droplets that what are shown would exceed the breakup criteria. These droplets above breakup criteria would be subject to breakup.

4. Conclusion

From an integrated study that is carried out, considering of nozzle geometry, internal flow inside nozzle and operating pressure conditions, the following observation can be made:

(1) The sharp entrance nozzle has smaller Sauter mean diameter and wider spray angle, which is partly due to the higher turbulence intensity at an exit plane near wall.

(2) At lower opening pressure with lower ambient pressure, a protrusion can be observed which might be injected into the chamber at the opening of the needle from the fuel in the sac volume of the injector.

(3) As increase of opening pressure spray tip penetration and spray angle were increased at both lower ambient pressure and higher ambient pressure.

(4) The increase of injection velocity changes the tip of the velocity profile and increases the number density of droplets that are likely to breakup due to the high relative velocity even though the droplet diameters are shifted lower ranges.

References

Chang, S. K. and Koo, J. Y., 1995, "Transient Liquid Breakup Model and Comparison with Phase Doppler Measurements," *KSME Journal*, Vol. 9, No. 1, pp. 41~50.

He, L. and Ruiz, F., 1995, "Effects of Cavitation on Flow and Turbulence in Plain Orifices for High-Speed Atomization," *Atomization and Spray*, Vol. 5, pp. 569~584.

Koo, J. Y. and Martin, J. K., 1995, "Near Nozzle Characteristics of a Transient Fuel Spray," *Atomization and Spray*, Vol. 5, No. 1, pp. 107~121.

Koo, J. Y., Oh, D. S. and Park, J. H., 1996, "Prediction of the Internal Flow in a Diesel Nozzle," The 3rd International Symposium on Aerodynamics of Internal Flows, Beijing, pp. 856~862.

Licharowicz, A. Duggins, R. K., Markaland, E., 1965, "Discharge Coefficients for Incompressible Non-Cavitating Flow Through a Long Ori-

fice," *Journal of Mech. Engr. Science*, Vol. 7, No. 2, pp. 201~219.

Oblander, K., Kollmamm, K., Kramer, M. and Kutschera, I., 1989, "The Influence of High Pressure Injection of Performance and Exhaust Emission of a High Speed Direct Diesel Engine," SAE Paper 890438.

Ohrn, T. R., 1989, "The Effect of Internal Geometry and Injection Pressure on the Flow and Spray Characteristics of a Plain Orifice Atomizer," M.S, Purdue Univ.

Reitz, R. D. and Bracco, F. B., 1979, "On the Dependence of Spray Angle and Other Spray Parameters on Nozzle Design and Operating Conditions," SAE paper 790494.

Reitz, R. D. and Diwakar, R., 1986, "Effects of Drop Breakup on Fuel Sparys," SAE paper 860469.

Ruiz, F., 1981, "A Few Useful Relations for Cavitating Orifices," ICLASS-91, pp. 595~602.

Shimizu, M., Arai, M. and Hiroyasu, H., 1990, "Disintegrating Progress of a Liquid Jet and Internal Flow in a Nozzle," *JSME*, Vol. 56, No. 528, pp. 2519~2525.

Wang, X. F., Chin, J. S. and Lefebvre, A. H., 1989, "Influence of Gas-Injector Geometry on Atomization Performance of Aerated-liquid Nozzles," *International Journal of Turbo and Jet Engine*, Vol. 6, pp. 271~291.